On the SNR Statistics in Coupled-Core Multi-Core Fiber Transmissions with Mode-Dependent Loss

Chiara Lasagni, *Member, IEEE,* Paolo Serena, *Senior Member, IEEE,* Alberto Bononi, *Senior Member, IEEE*, Lucas A. Zischler, *Student Member, IEEE,* Giammarco Di Sciullo, *Student Member, IEEE,* Antonio Mecozzi, *Fellow, IEEE, Fellow, Optica,* and Cristian Antonelli, *Senior Member, IEEE, Fellow, Optica*

***Abstract*—We investigate the impact of mode-dependent loss (MDL) on the statistics of the signal-to-noise ratio (SNR) in coupled-core multi-core fiber (CC-MCF) systems. Through numerical simulations, we present an in-depth analysis of the impact of MDL on received amplified spontaneous emission (ASE) noise and nonlinear interference (NLI), as well as their joint contribution to the SNR. We show that MDL induces different statistics on the two noises and discuss the differences with single-mode polarization-dependent loss. Moreover, we investigate the impact of spatial mode dispersion (SMD) on the MDL-induced impairment, offering insights on their joint effects on ASE and NLI.**

***Index Terms*—Space-division multiplexing, multi–core fibers, mode-dependent loss, nonlinear interference.**

I. Introduction

OPTICAL communication systems implementing space-division multiplexing (SDM) have the benefit of leveraging multiple light paths to increase capacity compared to standard single-mode fiber (SMF). Multi-core and multi-mode fibers, or combinations of the two, are common SDM options [1]. However, depending on the fiber design, the spatial paths may experience significant crosstalk, causing the signals propagating in each spatial path to become evenly mixed [2], [3]. This coupling regime occurs in multi-core fibers with narrow core separation, known as coupled-core multi-core fibers (CC-MCFs), and within mode groups of multi-mode fibers.

Manuscript received ******* **, 2026. This work has been supported by University of Parma through the action *Bando di Ateneo 2023 per la ricerca,* the Next Generation EU under the Italian National Recovery and Resilience Plan (NRRP), Mission 4, Component 2, Investment 1.3, CUP B53C22003970001, partnership on "Telecommunications of the Future" (PE00000001 - program "RESTART"), and by the European Union's Grant Agreement 101120422 - Quantum Enhanced Optical Communication Network Security (QuNEST).

C. Lasagni, P. Serena, and A. Bononi are with the Department of Engineering and Architecture, Università degli Studi di Parma, Parma, 43124, Italy, and with National Inter-University Consortium of Telecommunications - CNIT, Italy (e-mail: chiara.lasagni@unipr.it, paolo.serena@unipr.it; alberto.bononi@unipr.it).

L. A. Zischler, G. Di Sciullo, A. Mecozzi, C. Antonelli are with the Department of Physical and Chemical Sciences, Università degli Studi dell'Aquila, L'Aquila, 67100, Italy, and with National Inter-University Consortium of Telecommunications - CNIT, Italy (e-mail: giammarco.disciullo@graduate.univaq.it, lucas.zischler@univaq.it, antonio.mecozzi@univaq.it, cristian.antonelli@univaq.it).

Color versions of one or more of the figures in this paper are available online at http://xxxxxxxxxx.xxxx.xxx.

Digital Object Identifier xx.xxxx/JLT.xxxx.xxxxxxx

In the case of CC-MCFs, a multiple-input multiple-output (MIMO) equalizer is required to remove linear crosstalk and untangle the signals. Nevertheless, the strong coupling among the cores is beneficial in reducing the accumulation of impairments during propagation, such as spatial mode dispersion (SMD), mode-dependent loss (MDL), and nonlinear interference (NLI) [4]. The slower accumulation rate of SMD [5], ps/$\sqrt{\text{km}}$ rather than ps/km, is of particular relevance to reduce the complexity of the MIMO in terms of a reduced number of taps [6]. As a result, CC-MCFs have consistently shown the potential of achieving ultra-high data rates [7]–[11], also in deployed conditions [12], ultimately reaching the order of petabits per second [13].

The reduction of the accumulated MDL is an important factor at system level, as MDL is a major source of impairment limiting system capacity [14]–[16]. Mode-dependent loss refers to the different random losses/gains experienced by the polarizations and spatial modes propagating in the optical system [2], and it generalizes the concept of polarization-dependent loss (PDL) in single mode fibers to the multi-dimensional scenario of SDM. Sources of MDL span from optical fibers to multiplexers, amplifiers, and other optical devices [17]–[20], rendering essential a characterization of the link MDL for effective system design and operation [21], [22]. Contrary to mode dispersion, MDL cannot be completely removed by digital signal processing (DSP) [23]. For instance, even with zero-forcing equalization with perfect channel state information, MDL remains on the detected noises. In fact, as both amplified spontaneous emission (ASE) noise introduced by the amplifiers and the fiber NLI arise distributed along the link, they accumulate a different amount of MDL compared to the signal. As a consequence, MDL degrades the signal-to-noise ratio (SNR) and makes it a random variable inducing outage events on the system performance.

For these reasons, evaluating the impact of MDL on the system performance is crucial, and it has been the focus of several studies [6], [14], [15], [24]–[30]. However, in these studies, the NLI has been either neglected or treated as unaffected by MDL. Nevertheless, similar single-mode studies highlighted significant differences between the impact of PDL on the linear and nonlinear noise [31]–[33].

In this work, which extends our preliminary study in [34], we bridge this gap by investigating the impact of MDL and SMD on both ASE and NLI, thereby providing a comprehensive comparison of their impact on SNR statistics. Exploiting numerical split-step Fourier method (SSFM) simulations, we

study the MDL-induced statistics of the linear and nonlinear noise individually, to highlight the differences between the two noises. We first carry out the simulations in the absence of SMD, to focus solely on the effect of MDL. Then, we consider a more comprehensive scenario where both MDL and SMD impair the system, and we estimate the statistics of the SNR in different conditions.

The numerical approach adopted in this work offers significant insights into the impact of MDL on system performance, which are often hidden in the experiments. Furthermore, it allows to extend the analysis to the nonlinear regime in SDM links, which remains largely unexplored experimentally. However, the SSFM's numerical effort is significant, as it requires many runs to adequately sample the SNR statistics. For this reason, analytical or semi-analytical models are extremely useful in reducing the computation times in practical scenarios. In this paper, we also adapt the PDL-GN model, which was first published in [33] to study the impact of PDL on the NLI in SMF, to the case of CC-MCFs in a simplified scenario without SMD. This extension proves itself accurate against numerical simulations.

The paper is structured as follows. Section II provides an overview of MDL in optical systems based on CC-MCFs, offering comparisons with single-mode PDL. Section III focuses on the impact of MDL on the statistics of the SNR, with and without mode dispersion. Finally, Section IV presents our conclusions.

II. MDL IN CC-MCF SYSTEMS

The accumulation of MDL in an MCF-based link can be described through a waveplate model by generalizing the single-mode theory [36] to $2N$ dimensions [2], with N accounting for the number of cores and the factor 2 for polarization degeneracy. We divide the link into the concatenation of K independent sections. A section describes the MDL accumulated in a segment of the optical fiber or within an optical device, like an amplifier or a switch. Mode-dependent loss couples the $2N$ polarizations through a matrix $\mathbf{M}^{(k)}$, whose singular value decomposition (SVD) can be expressed as:

$$\mathbf{M}^{(k)} = e^{\frac{1}{2}\overline{g}^{(k)}}\mathbf{V}^{(k)}\mathbf{\Lambda}^{(k)}\mathbf{U}^{(k)\dagger}, \quad k = 1, \dots, K \tag{1}$$

where $\mathbf{V}^{(k)}$ and $\mathbf{U}^{(k)}$ are $2N \times 2N$ random unitary matrices representing random mode coupling at the beginning and end of the section, and the dagger denotes Hermitian conjugate. The uncoupled propagation of the field in each section is described by the diagonal matrix $\mathbf{\Lambda}^{(k)} = \mathrm{diag}[e^{\frac{1}{2}g_1^{(k)}}, \dots, e^{\frac{1}{2}g_{2N}^{(k)}}]$, where the gains satisfy $\sum_i g_i^{(k)} = 0$, as we factored out the average MDL $\overline{g}^{(k)}$ in (1).

The matrix $\mathbf{M}$ modeling the system MDL is given by the concatenation of the K section matrices, namely:

$$\mathbf{M} = \mathbf{M}^{(K)} \cdots \mathbf{M}^{(2)}\mathbf{M}^{(1)} = \mathbf{V}\mathbf{\Lambda}\mathbf{U}^{\dagger} \tag{2}$$

with $\mathbf{\Lambda} = \mathrm{diag}[e^{\frac{1}{2}g_1}, \dots, e^{\frac{1}{2}g_{2N}}]$, where we define the system MDL by the factors g_i, $i = 1, \dots, 2N$, which are the logarithm of the squared singular values of the total transfer matrix $\mathbf{M}$, or, equivalently, the logarithm of the eigenvalues of the MDL operator $\mathbf{M}\mathbf{M}^{\dagger} = \mathbf{V}\left(\mathbf{\Lambda}\right)^2\mathbf{V}^{\dagger}$ [14], [24].

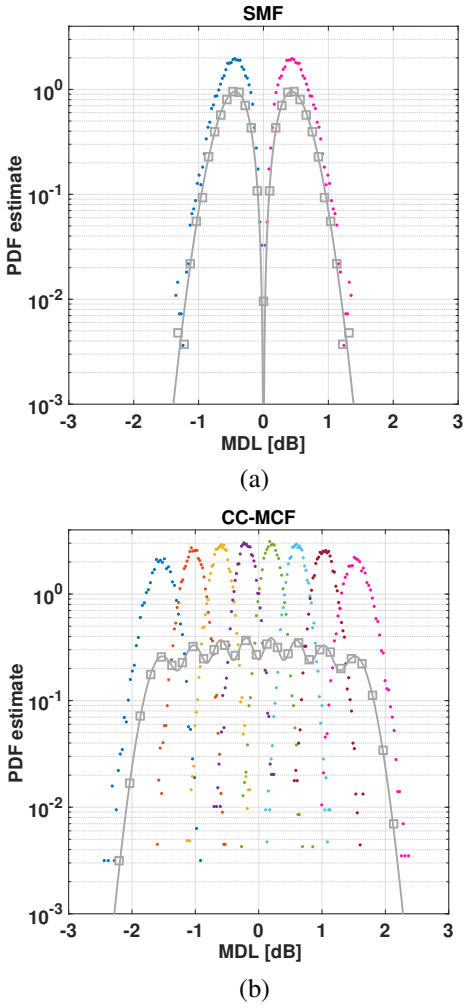

Fig. 1. Probability density function of the system MDL expressed in dB. Results obtained from 10^4 random realizations of the MDL transfer matrix, built by concatenation of $K = 256$ sections. Top: single core. Bottom: four strongly coupled cores. Squares: distribution of a randomly-picked singular value of $\mathbf{M}$. Dots: marginal distribution of the $2N$ order statistics. Solid lines: expressions from [14].

Equation (1) can be generalized to include mode dispersion. In this case, in the Fourier domain, the generic ith element on the main diagonal of the matrix $\mathbf{\Lambda}^{(k)}$ becomes frequency-dependent and equal to $e^{\frac{1}{2}g_i^{(k)} - j\omega\tau_i^{(k)}}$, with $\tau_i^{(k)}$ the time delay experienced by the i-the space and polarization mode in section k, and ω the angular frequency shift. In the case of lumped MDL, the total matrix in (2) is a concatenation of frequency-independent MDL matrices and MDL-free frequency-dependent fiber sections introducing mode dispersion.

Due to the random nature of each section, the system MDL impairing the polarizations is a random variable, whose distribution has been studied and approximated analytically both in SMF [37] and MCF [14] transmissions.

To better understand the differences between the single-core and multi-core scenarios, we implemented the previously described waveplate model to numerically estimate the probability density function (PDF) of the MDL in the two cases. Similar to [2], we considered a transmission along $K = 256$

sections with the same matrix $\mathbf{\Lambda}^{(k)}$ in each section, with $g_i^{(k)} = (-1)^i \sigma_g$. The value of σ_g was set to 0.014 in the four-core, and adapted to 0.0076 in the single-core case, in order to investigate both cases at the same MDL-induced reduction in average spectral efficiency per mode [24]. We verified that the adopted number of sections was sufficient to correctly capture the MDL statistics. We collected 10^4 random realizations of the MDL transfer matrix, and, for each realization, we estimated the system MDL from its singular values. Figure 1 shows with square markers the PDF of a randomly selected singular value of $\mathbf{M}$, i.e., the mixture distribution. The dotted PDFs refer to the $2N$ singular-values order statistics, i.e., the smallest (leftmost) up to the largest (rightmost) singular values. The top figure refers to a single core while the bottom to four strongly-coupled cores.

In the single-core case, the two marginal PDFs in Fig. 1(a) refer to the smallest and largest singular value, which, depending on the specific realization, can impair either the x or y polarization. Therefore, as one polarization gains power, the other is attenuated, resulting in a clear difference between the best and worst polarization. Figure 1(a) also shows that the numerical PDF of the MDL agrees with the analytical two-sided Maxwellian distribution (solid line) [37].

In the multi-core case, due to the strong coupling among space and polarization modes, the PDF of the MDL exhibits a different shape compared to the Maxwellian distribution observed in the single-core case. Namely, the mixture distribution has a multimodal distribution with $2N=8$ peaks, in agreement with the analytical expression reported in [14] (solid line), and the experimental measurements shown in [38]. It is worth noting that the dotted PDFs refer to the singular-value order statistics and not to the individual polarizations in the cores. As a consequence, the two polarizations of a given core may not have symmetric PDFs as in the SMF case, and they may both experience a gain or a loss.

Despite the useful insights provided by the MDL PDF, at a system level the MDL is often quantified in terms of standard deviation σ_{MDL} of the generic element g_i, $i = 1, \ldots, 2N$, or mean peak-to-peak MDL [22], [28]. The latter metric is defined as the mean of the $10\log_{10}(\cdot)$ of the ratio between the maximum and minimum squared singular values of the system matrix $\mathbf{M}$ [14]:

$$\begin{aligned}\langle \mathrm{MDL_{dB}} \rangle &= \left\langle 10\log_{10}\left(e^{(g_{\max}-g_{\min})}\right)\right\rangle \\ &= 4.343\,\langle (g_{\max}-g_{\min})\rangle\end{aligned} \tag{3}$$

with $\langle\cdot\rangle$ denoting ensemble averaging.

III. Impact of MDL on the Signal-to-Noise Ratio

Assuming ASE and NLI as independent additive noises, the SNR of a generic frequency channel in a given core can be conveniently expressed as:

$$\frac{1}{\mathrm{SNR}} = \frac{N_x + N_y}{P_x + P_y} = \frac{1}{\mathrm{SNR_{ASE}}} + \frac{1}{\mathrm{SNR_{NLI}}} \tag{4}$$

where $N_{x,y}$ and $P_{x,y}$ represent the noise and signal power in the x and y polarization. $\mathrm{SNR_{ASE}}$ and $\mathrm{SNR_{NLI}}$ are the linear and nonlinear SNR accounting only for ASE or NLI as a source of noise, respectively. The presence of MDL changes the ASE and NLI power as they accumulate MDL differently compared to the signal. This concept is sketched in Fig. 2, for the simple case of a two-span system with lumped MDL at each span end. The figure highlights that, contrary to the ASE noise w_i, the NLI n_i arising in the ith span depends on the signal A and, thus, on the MDL at previous coordinates. Such dependency is a key factor that distinguishes the two types of noise. It is represented in the figure through the nonlinear operator $\mathcal{N}(A)$ which, under perturbative assumptions, can be reasonably approximated by a multilinear (cubic) map of the individual signal frequencies entering the span [39], [40].

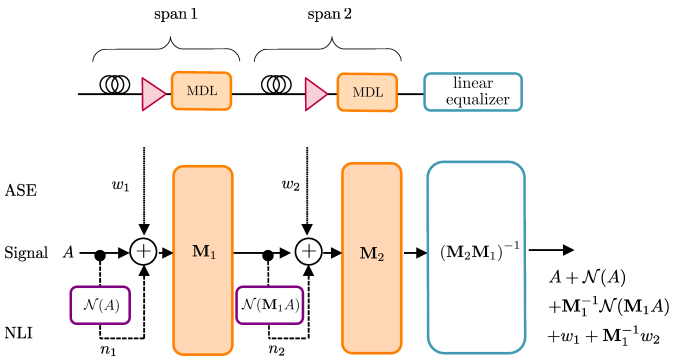

Fig. 2. Schematic MDL accumulation in a two-span optical system with lumped MDL and zero-forcing linear equalization. A: signal. w_i and n_i: ASE noise and perturbative NLI, respectively, arising in the ith span.

To investigate the different impact of the residual MDL on ASE and NLI after signal equalization, we focused on three scenarios: i) only ASE, ii) only NLI, iii) ASE + NLI. We considered the transmission of independent wavelength-division multiplexed (WDM) signals in each core of a 10×100 km optical link based on CC-MCFs with $N=4$ cores and lumped MDL after each span. Fiber propagation was implemented using SSFM simulations solving the Manakov equation for CC-MCFs [4]. The fiber under test had core-independent attenuation 0.2 dB/km, chromatic dispersion 17 ps/(nm·km), and nonlinear coefficient $1.267/N = 0.3167$ 1/(W·km). The fiber SMD coefficient varied depending on the system configuration. The amplifiers had frequency flat gain of 20 dB and noise figure equal to 6 dB.

To emulate the MDL introduced by an amplifier, we placed an MDL element at each span end, as shown in Fig. 3. The MDL element was modeled by cascading a frequency-independent matrix, as described in Sec. II, and a noiseless amplifier equalizing the mode-averaged loss. Each MDL element had peak-to-peak MDL of 1 dB ($\sigma_g^2 = 0.015$, with $g_i^{(k)} = (-1)^i \sigma_g$), yielding a link peak-to-peak MDL of 4.8 dB according to (3). Following the observations in [5], we neglected the MDL induced by the optical fiber, focusing instead on the larger MDL contributions from optical components.

We considered the transmission of a WDM signal composed of five dual-polarization channels per core, with a symbol rate of 64 Gbaud and channel spacing of 75 GHz. We transmitted sequences of 65536 complex Gaussian distributed symbols, well above the number required by the maximum channel walk-off, to improve the accuracy of Monte Carlo estimations.

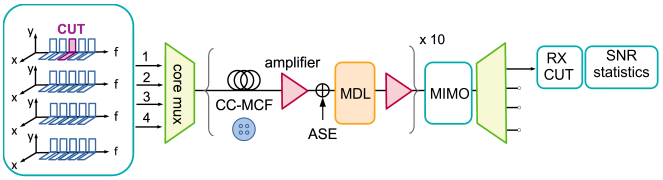

Fig. 3. Sketch of the transmission under test. Five dual-polarizarion WDM channels transmitted in each core of 100-km four-core CC-MCFs. The MDL is applied at span end, with the last amplifier recovering the mode-averaged loss. After ten identical spans, ideal equalization of the linear effects and coherent detection are performed, and the SNR of the channel under test is estimated for each MDL realization.

The dual-polarization power $P_x + P_y$ of each WDM channel power was set to 5 dBm, corresponding to the nonlinear threshold value maximizing the SNR in the absence of MDL and SMD.

At the receiver, we optically compensated all linear effects accumulated during propagation by inverting the channel transfer matrix. After the detection of the dual-polarization channel under test (CUT) and compensation of the average phase rotation accumulated during fiber propagation, we estimated the CUT SNR from the received constellation. As depicted in Fig. 3, the CUT was the central WDM channel of core 1. We analyzed a single core to facilitate comparison with SMF. The statistical equivalency of the remaining cores, and the core-averaged SNR behavior, is discussed in the next section.

Mode dispersion, when present, was implemented with the waveplate model of the optical fiber described in Sec. II with 100-m long waveplates. For each configuration of link parameters, the step was updated with the constant local error criterion [41]. The initial step was halved until ten seeds of the detected SNR reached saturation within 0.05 dB after the first 100-km span, ranging from 500 m to 125 m depending on the scenario under test.

In the absence of SMD, we also adopted the semi-analytical Gaussian noise (GN) model in [33] to estimate the PDF of the SNR. Although this model was originally proposed and validated for single-mode transmissions in the presence of PDL, thanks to the strong coupling among the cores, it can be applied as well in our scenario by adapting it to a higher dimension of $2N$ space and polarization modes.

A. SNR statistics without mode dispersion

As a preliminary investigation, we studied the SNR statistics in the absence of SMD, which is more representative of SMF transmission rather than CC-MCF. Figure 4(a) shows, for the CC-MCF, the PDF of the SNR in the three cases under test, i.e., linear, nonlinear, and total SNR. We normalized the SNR to its mean value to ease the comparison among the three distributions, namely:

$$\Delta\text{SNR}\,[\text{dB}] \triangleq \text{SNR}\,[\text{dB}] - \langle \text{SNR}\,[\text{dB}] \rangle\,. \tag{5}$$

Markers indicate results from SSFM simulations, while solid lines represent semi-analytical estimations provided by the PDL-GN model [33]. The model and the SSFM results are

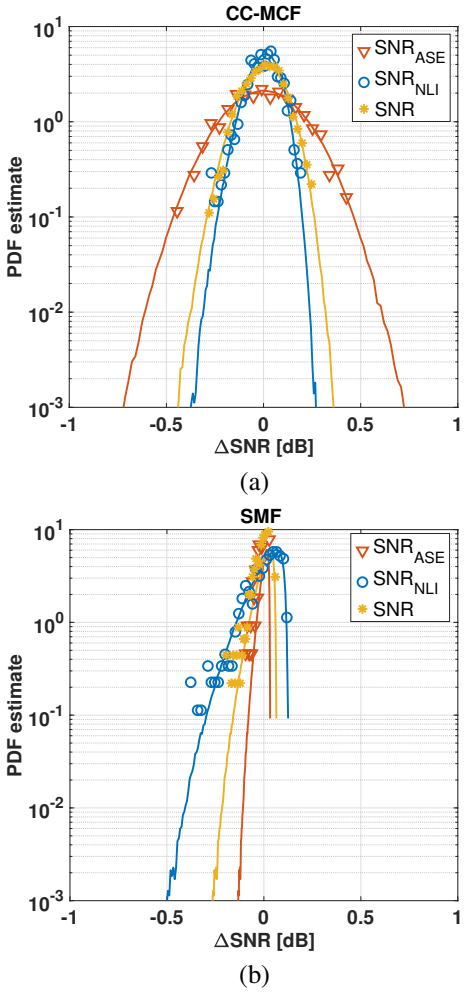

Fig. 4. PDF of ΔSNR, i.e., SNR deviation from its mean, for the three cases under test in the absence of SMD. Top (a): core 1 of a four-core CC-MCF, peak-to-peak MDL of each amplifier equal to 1 dB. Bottom (b): SMF, peak-to-peak PDL of each amplifier equal to 0.5 dB. Markers: PDF estimated from SSFM results. Solid lines: PDL-GN model [33] results. Channel power set to maximize the SNR, in the absence of MDL, in both setups.

remarkably in agreement with each other. However, it is worth noting that we simulated 500 realizations with SSFM owing to the computational complexity, while the semi-analytical model performed substantially faster, allowing us to test 10^6 seeds.

The different distributions of the linear and nonlinear SNR reported in the figure indicate different interactions of MDL with the NLI and ASE noise. In particular, the figure shows that the MDL causes greater random variations in the linear SNR compared to the nonlinear one. This observation is in contrast with the results reported in the literature for SMF transmissions [32], [33]. To explore this discrepancy, we performed simulations with SMF fibers as well. The lumped peak-to-peak MDL (here PDL) of each element was set to 0.5 dB. This choice ensures the same MDL-induced reduction in average spectral efficiency per mode, in the linear regime, for both the SMF and CC-MCF [24]. The channel power was decreased to its optimal value equal to 3 dBm. Figure 4(b) shows, for the SMF, the PDFs of the linear, nonlinear, and total SNR obtained with numerical simulations and the semi-

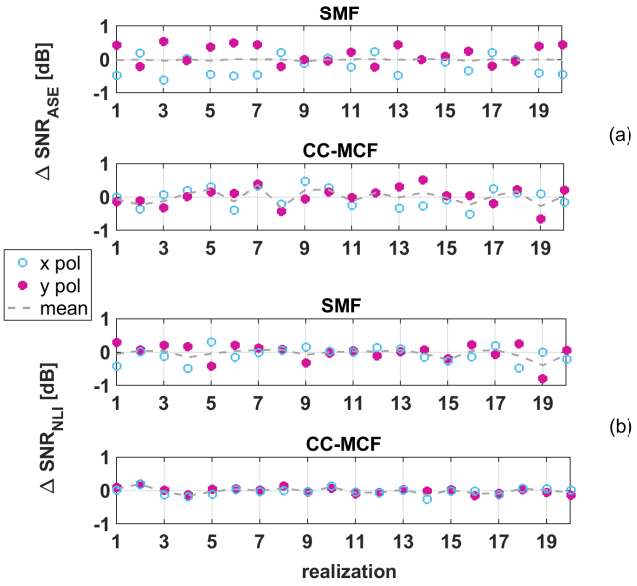

Fig. 5. Markers: deviation from the mean of the per-polarization SNR of the core under test in different random realizations, in the linear (a) and nonlinear (b) case. Dashed line: average between polarizations. Estimations obtained with the semi-analytical PDL-GN model.

analytical model.

Comparing the distributions in Fig. 4, it is evident that the PDFs of the SNR in the CC-MCF link exhibit less skewness compared to the SMF case, both in linear and nonlinear regime. A qualitative explanation of this difference can be obtained by noting that the PDFs of the ordered singular values of the MDL matrix $\mathbf{M}$ (the dotted curves in Fig. 1) in turn exhibit less skewness in the MCF case compared to the SMF.

Another important difference emerging from the comparison between the PDFs in Fig. 4 is the smaller standard deviation in the SMF case, compared to the multi-core case. To gain insight into this difference, we start by analyzing the linear SNR, that is $\mathrm{SNR}_{\mathrm{ASE}}$. Figure 4 shows that the SMF case has a smaller standard deviation than the CC-MCF by a factor of 8.6. The narrower PDF in the SMF case can be explained considering the differences in the distributions of the MDL singular values in Fig. 1. While the single-mode PDL increases the ASE power in one polarization, it depletes the other following a symmetric bimodal distribution. As a confirmation of this phenomenon, Fig. 5 (a) shows that the $\mathrm{SNR}_{\mathrm{ASE}}$ deviations from the mean exhibit antithetic behavior in the two polarizations, leading to a fairly steady zero polarization-averaged value across realizations (dashed line). As a consequence, the PDFs of the linear SNR of the best- and worst-performing polarization exhibit antithetic tails, as shown in Fig. 6(a). In contrast, in the CC-MCF case, all the cores are mixed together, resulting in no compensation between the polarizations within each core, as anticipated in Sec. II. Consequently, the linear SNR of the two polarizations in a given core may both decrease or increase. This lack of mutual compensation gives rise to a non-zero polarization-average ΔSNR, as shown in the bottom panel of Fig. 5(a). As a result, the PDFs of the best and worst

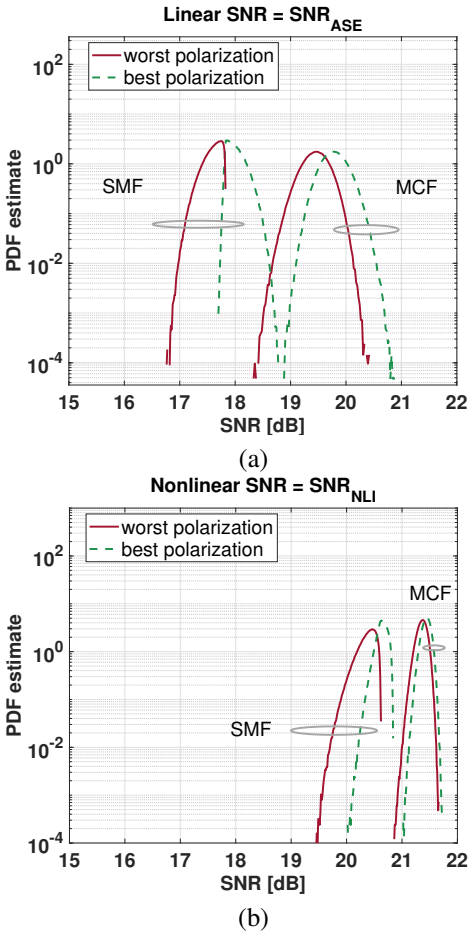

Fig. 6. PDF of linear (a) and nonlinear (b) SNR of the best and worst polarization of the core under test, for the same scenario of Fig. 4, obtained with the model in [33]. Solid lines: four-core CC-MCF. Dashed lines: SMF.

polarization in core 1 have comparable shapes.

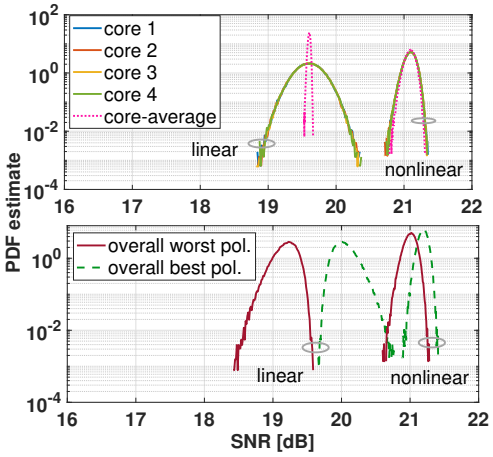

Fig. 7. Top: PDF of linear and nonlinear SNR of each core of the CC-MCF fiber (solid) and core-averaged SNR (dotted). Bottom: PDF of the SNR of the best and worst polarization among all the cores.

In the nonlinear regime, the $\mathrm{SNR}_{\mathrm{NLI}}$ deviations of the best and worst polarization in one core do not average to zero in each realization, as shown in Fig. 5(b). This can be attributed

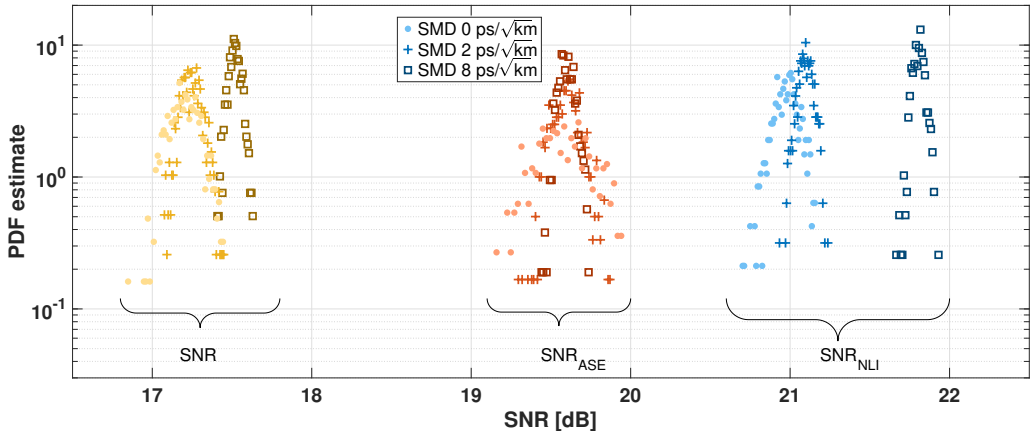

Fig. 8. PDF of linear (center), nonlinear (right), and total (left) SNR of core 1 estimated from SSFM results collecting 500 channel realizations. 10×100 km link of MCF with four coupled cores, and peak-to-peak MDL of each amplifier equal to 1 dB. Fiber SMD coefficient equal to: 0 (dots), 2 (crosses), and 8 (squares) ps$/\sqrt{\text{km}}$. Transmitted WDM signal: five channels spaced 75 GHz with symbol rate equal to 64 Gbaud and power 5 dBm.

to the different characteristics of the NLI compared to the ASE noise. In particular, it is worth noting that the self- and cross-phase modulation contributions (SPM and XPM, respectively) to the NLI represent a scalar impairment which, despite the MDL-induced unbalances, is common to all polarizations [32] and depends on the total power across the cores. As a result, the nonlinear SNR of the best and worst polarization exhibit comparable, although shifted, distributions, as shown in Fig. 6(b). In the SMF case, this leads to a wider PDF of the non-linear SNR compared to the linear case, where the symmetry between the two polarizations allows for mutual compensation thus mitigating the SNR fluctuations. Conversely, in the MCF case, where such a symmetry is absent at a core level even in the linear regime, the total power dependence of the NLI effectively renders the nonlinear SNR PDF narrower than the linear one. It is worth noting that, as explored in [34], this behavior persists even when comparing the two scenarios at the same value of MDL and PDL. Additional simulations further confirmed that these findings extend beyond the four-core scenario.

For completeness, Fig. 7 shows the PDF of the linear and nonlinear SNR of each core of the CC-MCF, as well as the PDF of the core-averaged SNR. It can be seen that, thanks to the strong linear mixing, all the cores are statistically equivalent, although not independent. The bottom panel of the figure shows that, when evaluated across all the coupled cores, the PDFs of the worst- and best-performing polarization exhibit antithetic tails in the linear regime. This behavior is consistent with theSMF case, resulting in vanishing deviations of thecore-averaged SNR reported in the top panel. On the contrary, the PDF of the core-averaged nonlinear SNR is similar to that of the per-core case due to the absence of compensation among the MDL-induced deviations.

For the sake of comparison, we tested the GN model under quasi-distributed scenario where the per-span MDL was distributed across the fiber length through an increasing number of MDL elements, while keeping the total system MDL constant. We observed negligible variations in the SNR statistics with respect to the lumped case, suggesting that a lumped MDL per span is sufficient to replicate a distributed scenario after ten spans, thereby ensuring the generality of the results.

The results reported in this section were obtained neglecting mode dispersion, whose effect is to make the system MDL frequency-dependent. Such phenomenon, often referred to as frequency diversity [28], [42], tends to average out MDL due to its random fluctuations across the channel bandwidth. Nevertheless, the extent of this effect on the power of the NLI remains unclear. Therefore, the next section will focus on estimating the SNR statistics using SSFM simulations that include both SMD and MDL.

B. SNR statistics with mode dispersion

To investigate the combined effect of MDL and SMD on the SNR statistics, we repeated the SSFM simulations including the SMD in the optical fiber and full linear impairment compensation before detection, for the same 10×100 km link.

The PDFs of the linear, nonlinear, and total SNR of core 1 are reported in Fig. 8. The results obtained with an SMD coefficient of 2 ps$/\sqrt{\text{km}}$ are represented with crosses, while squares indicate the case of 8 ps$/\sqrt{\text{km}}$. For comparison, we reported in the same figure the PDFs obtained in the absence of SMD (dots). The figure shows that, in all the cases, the SNR distributions remain Gaussian-like in the presence of mode dispersion. Nevertheless, the differences among the displayed PDFs indicate that the SMD affects differently the mean and standard deviation of the SNR in the linear and nonlinear regime. This marks a significant difference compared to the single-mode case, where the small value of the PMD coefficient in typical SMF fibers has negligible impact on the SNR distribution [33].

It is important to note that our results were based on a zero-forcing optical MIMO equalization rather than a least squares or minimum mean square error equalizers [21], [29], [30]. To assess the impact of this technique for the setup under test, we performed additional simulations with a least-squares

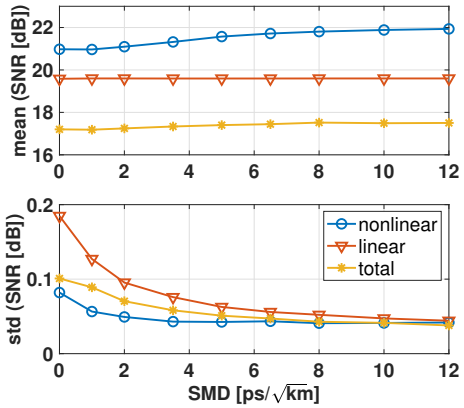

Fig. 9. Standard deviation and mean value of the SNR as a function of the SMD coefficient, estimated from SSFM results. Peak-to-peak MDL of each amplifier equal to 1 dB.

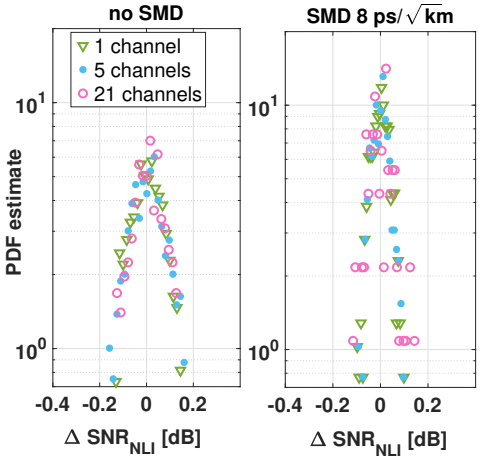

Fig. 10. PDF of the nonlinear SNR deviation from its mean with SMD coefficient 0 ps/$\sqrt{\text{km}}$ (left) and 8 ps/$\sqrt{\text{km}}$ (right). Variable number of WDM channels: 1 (triangles), 5 (dots), 21 (circles), with channel power 5.5 dBm, 5 dBm, and 4.6 dBm, respectively. Fixed symbol rate of 64 Gbaud and channel spacing 75 GHz. Peak-to-peak MDL of each amplifier equal to 1 dB.

digital MIMO approach finding no substantial difference in the SNR statistics with respect to the results shown in Fig. 8. However, in low-SNR scenarios combined with high MDL, the zero-forcing approach can lead to significant performance degradation due to noise enhancement [21], [29].

To better highlight the role of mode dispersion in setting the SNR statistics, in Fig. 9 we report the standard deviation and mean value of the linear, nonlinear, and total SNR as a function of the SMD coefficient, extending the range up to 12 ps/$\sqrt{\text{km}}$. Figure 9 shows that the mean SNR is affected by mode dispersion only in the presence of fiber nonlinearity. Namely, the nonlinear SNR increases thanks to the beneficial effect of the SMD in mitigating the accumulation of the NLI along the distance. Such an observation is in agreement with the findings of [39], [43], where the effect of SMD on the NLI was investigated neglecting the MDL.

Figure 9 also shows that the SMD is effective in reducing the standard deviation of the linear SNR. This behavior is due to the random SMD-induced frequency fluctuations in the mode-dependent gains/losses, which result in a beneficial averaging effect [6], [14], [28]. As a result, the random deviations of the ASE noise in core 1 are reduced, leading to the shrinkage of the linear SNR PDF shown in Fig. 8. Such a frequency diversity phenomenon is still present in the nonlinear noise, yet less evident. The results indicate that the standard deviation of nonlinear SNR quickly saturates for moderate values of the SMD coefficient.

We observed that such behavior persists for different WDM bandwidths, by comparing simulation results obtained with 1, 5, and 21 channels. Figure 10 shows the PDF of the nonlinear SNR, normalized to its average value, obtained with an SMD coefficient equal to 0 ps/$\sqrt{\text{km}}$ (left) and 8 ps/$\sqrt{\text{km}}$ (right). For a given SMD coefficient, the PDFs are comparable, indicating that the inter-channel NLI (such as XPM and four-wave mixing) has little effect on the PDF width.

To verify the generality of these findings, we extended our analysis to a seven-core CC-MCF. We repeated the simulations of Fig. 8, adapting the MDL value per amplifier to 1.2 dB to match the average per-mode capacity reduction, and increased the channel power to 5.5 dBm to maximize the SNR. Figure 11 confirms that the behaviors observed for the four-core CC-MCF persists at a higher core count, with SMD reducing the random fluctuations in the core SNRs while increasing the average nonlinear SNR.

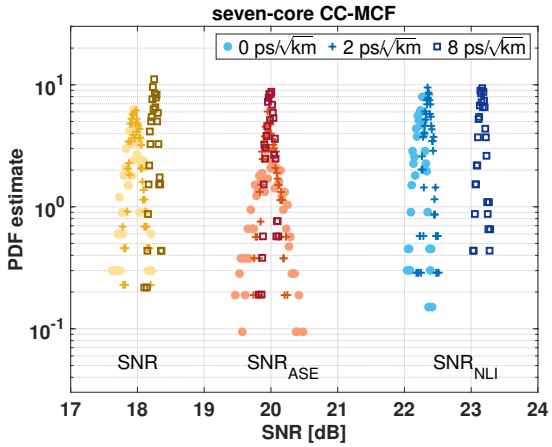

Fig. 11. PDF of linear (center), nonlinear (right), and total (left) SNR estimated from SSFM results collecting 500 channel realizations. 10 × 100 km link of MCFs. Fiber SMD coefficient equal to: 0 (dots), 2 (crosses), and 8 (squares) ps/$\sqrt{\text{km}}$. Transmitted WDM signal: five channels spaced 75 GHz with symbol rate equal to 64 Gbaud and power 5.5 dBm. Seven-core CC-MCFs with peak-to-peak MDL of each amplifier adapted to 1.2 dB.

We next investigated the impact of the per-amplifier MDL value on the SNR statistics at a fixed SMD coefficient of 2 ps/$\sqrt{\text{km}}$. Figure 12 shows the standard deviation and the mean value of the SNR in the three cases under investigation as a function of the amplifiers' MDL. In particular, we note that the standard deviation without MDL, i.e., caused by mode dispersion alone, is negligible both in the linear and nonlinear regimes. Therefore, despite the random nature of the SMD, the primary cause of SNR fluctuations can be attributed to MDL. The results also show different growth rates of the standard

TABLE I
SUMMARY OF KEY FINDINGS ON THE PER-CORE SNR ACROSS ANALYZED SYSTEMS.

	PDF of SNR	MDL-induced random fluctuations	SNR behavior with mode dispersion	
SMF	skewed	std(NLI) > std(ASE)	unaffected by practical values	
CC-MCF	symmetric	std(NLI) < std(ASE)	SNR_{NLI}: · decreased std · increased mean	SNR_{ASE}: · decreased std · unaffected mean

deviation of the two noises with the MDL magnitude. It is worth noting that the range of MDL values tested here is in line with measured peak-to-peak MDL values in the context of strongly coupled systems. As an example, [18] reported an MDL below 3 dB at 1550 nm for a seven-core CC-EDFA, [19] showed an MDL below 2 dB for a single span of a deployed four-core CC-MCF, and the measurements in [7] for a four-core CC-MCF system are consistent with a per-span MDL below 1 dB.

Figure 12 also highlights the detrimental impact of MDL on the mean SNR, showing a decrease of nearly 2.5 dB in the total mean SNR when each amplifier introduces 3 dB of peak-to-peak MDL. These results show that, while MDL is random, it eventually manifests in the detected signal as a nearly deterministic degradation of the SNR, particularly in the presence of SMD. These results, which include NLI, are in line with the observations made in the linear regime [6], [14], [27].

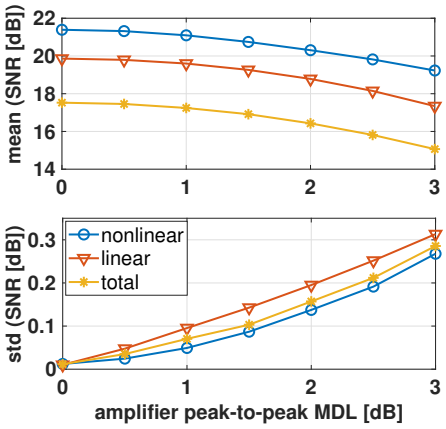

Fig. 12. Standard deviation and mean value of the SNR as a function of the peak-to-peak MDL of each link amplifier, estimated from SSFM results, with fixed SMD coefficient of 2 $ps/\sqrt{km}$.

IV. COMMENTS AND CONCLUSIONS

Mode-dependent loss is one of the most relevant propagation effects that limit the capacity of SDM systems. Several experiments have shown that different optical devices in the link may contribute significantly to the accumulation of MDL. Understanding this phenomenon is therefore essential for enhancing the capacity of SDM links. In this work, we explored this problem from different perspectives, from an analysis of the different implications of MDL on ASE and Kerr effect, to an investigation on the role of SMD on the SNR statistics. We leveraged the flexibility of a numerical analysis to isolate the Kerr contribution, namely the NLI, and analyzed the physics of its interplay with MDL.

The main findings of this work are summarized in Tab. I. Our results show that the fluctuations in the per-core SNR induced by MDL are primarily due to the interaction between MDL and ASE rather than MDL and NLI when the system is operated at the nonlinear threshold, contrary to what has been observed in the literature for polarization-dependent loss in SMFs. In addition, they revealed that the SNR predictability is enhanced in the presence of SMD, thanks to its frequency-averaging effect on MDL. Finally, we confirmed that SMD, when equalized at the MIMO receiver, improves the SNR by mitigating the Kerr effect even in the presence of MDL.

Such behaviors were observed both in a four- and seven-core CC-MCF, suggesting a minor dependence on the core count in the strong-coupling regime.

REFERENCES

[1] B. J. Puttnam, G. Rademacher, and R. S. Luís, "Space-division multiplexing for optical fiber communications," *Optica,* vol. 8, no. 9, pp. 1186–1203, 2021.
[2] K.-P. Ho and J. M. Kahn, "Mode coupling and its impact on spatially multiplexed systems," in *Optical Fiber Telecommunications VI B*, Amsterdam, The Netherlands: Elsevier, 2013.
[3] R. Ryf and C. Antonelli, "Space-division Multiplexing," in Springer *Handbook of Optical Networks*, B. Mukherjee, I. Tomkos, M. Tornatore, P. Winzer, and Y. Zhao, Eds. Cham: Springer International Publishing, 2020, pp. 353–394.
[4] C. Antonelli, M. Shtaif, and A. Mecozzi, "Modeling of nonlinear propagation in Space-Division Multiplexed fiber-optic transmission", *J. Light. Technol.,* vol. 34, no. 1, pp. 36–54, 2016.
[5] T. Hayashi et al., "Randomly-Coupled Multi-Core Fiber Technology", *Proc. IEEE*, vol. 110, no. 11, pp. 1786–1803, 2022.
[6] C. Antonelli, A. Mecozzi, M. Shtaif, N. K. Fontaine, H. Chen, and R. Ryf, "Stokes-Space Analysis of Modal Dispersion of SDM Fibers with Mode-Dependent Loss: Theory and Experiments", *J. Light. Technol.,*, vol. 38, no. 7, pp. 1668–1677, 2020.
[7] R. Ryf et al., "Coupled-core transmission over 7-core fiber", in *Proc. Optical Fiber Communication Conference Postdeadline Papers 2019, Optica Publishing Group*, San Diego, California, USA, 2019, paper Th4B.3.
[8] S. Beppu, D. Soma, H. Takahashi, N. Yoshikane, I. Morita and T. Tsuritani, "85.2-Tbit/s Coupled 4-Core Fiber Transmission over 3,120 km Using PS-16QAM Signals," in *Proc. 2021 Opto-Electronics and Communications Conference (OECC)*, Hong Kong, 2021, paper M3F.4.
[9] G. Rademacher et al., "High Capacity Transmission in a Coupled-Core Three-Core Multi-Core Fiber," *J. Light. Technol.*, vol. 39, no. 3, pp. 757–762, 2021.

[10] G. Rademacher et al., "A Comparative Study of Few-Mode Fiber and Coupled-Core Multi-Core Fiber Transmission," *J. Light. Technol.,* vol. 40, no. 6, pp. 1590–1596, 2022.

[11] A. Kawai et al., "Towards Petabit Per Second in Field: Ultrahigh-Capacity Terrestrial Transmission System with Coupled-Core Multi-Core Fibers," *J. Light. Technol.,* vol. 43, no. 13, pp. 6058–6070, 2025.

[12] R. S. Luís et al., "19.2 THz S+C+L Transmission in a Field Deployed, Randomly-Coupled, Multicore Fiber," in P*roc. European Conference on Optical Communications (ECOC),* Copenhagen, Denmark, 2025, paper M03.05.2.

[13] R. S. Luís et al., "1.02 Petabit/s Transmission Over 1,808.1 km in a 19-Core Randomly-Coupled Multicore Fiber," in P*roc. Optical Fiber Communication Conference (OFC) Postdeadline Papers 2025, Postdeadline Paper Digest (Optica Publishing Group, 2025)*, paper Th4A.1.

[14] K.-P. Ho and J. M. Kahn, "Mode-dependent loss and gain: statistics and effect on mode-division multiplexing", *Opt. Express*, vol. 19, no. 17, pp. 16612–16635, 2011.

[15] C. Antonelli, A. Mecozzi, M. Shtaif, and P. J. Winzer, "Modeling and performance metrics of MIMO-SDM systems with different amplification schemes in the presence of mode-dependent loss", *Opt. Express*, vol. 23, no. 3, pp. 2203–2219, 2015.

[16] S. Beppu, D. Soma, N. Yoshikane, and T. Tsuritani, "Dependence of Q2 on inter-core skew and mode-dependent loss in long-haul coupled-core multicore fibre transmission", in *Proc. European Conference on Optical Communications (ECOC)*, Switzerland, Basel, 2022, paper Th1D.4.

[17] M. Arikawa, K. Nakamura, K. Hosokawa, and K. Hayashi, "Long-Haul WDM/SDM Transmission Over Coupled 4-Core Fiber With Coupled 4-Core EDFA and Its Mode Dependent Loss Characteristics Estimation", *J. Light. Technol.,*, vol. 40, no. 6, pp. 1664–1671, 2022.

[18] M. Mazur et al., "Transfer Matrix Characterization and Mode-Dependent Loss Optimization of Packaged 7-Core Coupled-Core EDFA," in *Proc. 2021 European Conference on Optical Communication (ECOC)*, Bordeaux, France, 2021.

[19] M. Mazur et al., "Transfer Matrix Characterization of Field-Deployed MCFs," in *Proc. 2020 European Conference on Optical Communications (ECOC)*, Brussels, Belgium, 2020.

[20] G. Rademacher et al., "Peta-bit-per-second optical communications system using a standard cladding diameter 15-mode fiber," *Nat. Commun.,* 12, 4238, 2021.

[21] R. S. B. Ospina et al., "Digital Signal Processing for MDG Estimation in Long-Haul SDM Transmission," *J. Light. Technol.,* vol. 42, no. 3, pp. 1075–1084, 2024.

[22] K. Choutagunta, S. O. Arik, K.-P. Ho, and J. M. Kahn, "Characterizing Mode-Dependent Loss and Gain in Multimode Components," *J. Light. Technol.*, vol. 36, no. 18, pp. 3815–3823, 2018.

[23] M. Shtaif, "Performance degradation in coherent polarization multiplexed systems as a result of polarization dependent loss," *Opt. Express*, vol. 16, pp. 13918–13932, 2008.

[24] A. Andrusier, M. Shtaif, C. Antonelli, and A. Mecozzi, "Assessing the effects of mode-dependent loss in space-division multiplexed systems," *J. Light. Technol.,* vol. 32, no. 7, pp. 1317–1322, 2014.

[25] P. J. Winzer and G. J. Foschini, "MIMO capacities and outage probabilities in spatially multiplexed opti- cal transport systems," *Opt. Express*, vol. 19, no. 17, pp. 16 680–16 696, 2011.

[26] M. Arikawa et al., "Transoceanic-Class WDM/SDM Transmission of PDM-QPSK Signals Over 12-Coupled-Core Fiber," *J. Light. Technol.,* vol. 43, no. 4, pp. 1926–1933, 2025.

[27] L. A. Zischler and D. A. A. Mello, "Analytic Models for the Capacity Distribution in MDG-Impaired Optical SDM Transmission," *J. Light. Technol.,* vol. 43, no. 12, pp. 5558–5568, 2025.

[28] D. A. A. Mello, H. Srinivas, K. Choutagunta, and J. M. Kahn, "Impact of Polarization- and Mode-Dependent Gain on the Capacity of Ultra-Long-Haul Systems," *J. Light. Technol.,* vol. 38, no. 2, pp. 303–318, 2020.

[29] L. A. Zischler and D. A. A. Mello, "SDM Optical Systems With MMSE Equalizers: Information Rates and Performance Monitoring," *J. Light. Technol.*, vol. 43, no. 15, pp. 7119–7129, 2025.

[30] R. Gholamipourfard, A. Ghazisaeidi and R. S. B. Ospina, "A Complexity-Aware Theoretical Framework for the Performance Analysis of Linear MIMO Equalizers in Coherent Spatial-Division Multiplexing Transmission Systems," *J. Light. Technol.,* vol. 43, no. 11, pp. 5189–5201, 2025.

[31] N. Rossi, P. Serena and A. Bononi, "Polarization-Dependent Loss Impact on Coherent Optical Systems in Presence of Fiber Nonlinearity," *IEEE Photon. Technol. Lett.*, vol. 26, no. 4, pp. 334–337, 2014.

[32] N. Rossi, S. Musetti, P. Ramantanis, and S. Almonacil, "The Impact of Kerr Nonlinearity on the SNR Variability Induced by Polarization-Dependent Loss", *J. Light. Technol.*, vol. 37, no. 19, pp. 5048–5055, 2019.

[33] P. Serena, C. Lasagni, and A. Bononi, "The Enhanced Gaussian Noise Model Extended to Polarization-Dependent Loss," *J. Light. Technol.,* vol. 38, no. 20, pp. 5685–5694, 2020.

[34] C. Lasagni, P. Serena, A. Bononi, A. Mecozzi and C. Antonelli, "Investigation of Mode-Dependent Loss in Coupled-Core Multi-Core Fiber Transmissions with Fiber Nonlinearities," in *Proc. 50th European Conference on Optical Communication*, Frankfurt, Germany, 2024, paper Tu3B3.

[35] P. Poggiolini, "The GN model of non-linear propagation in uncompensated coherent optical systems," *J. Light. Technol.,* vol. 30, no. 24, pp. 3857–3879, 2012.

[36] J. N. Damask, *Polarization Optics in Telecommunications*. New York, NY, USA: Springer, 2005.

[37] M. Karlsson and M. Petersson, "Quaternion Approach to PMD and PDL Phenomena in Optical Fiber Systems," *J. Light. Technol.*, vol. 22, no. 4, pp. 1137–1146, 2004.

[38] M. Cappelletti et al., "Statistical Analysis of Modal Dispersion in Field-Installed Coupled-Core Fiber Link," *J. Light. Technol.,* vol. 42, no. 11, pp. 4103–4109, 2024.

[39] P. Serena, C. Lasagni, A. Bononi, C. Antonelli, and A. Mecozzi, "The Ergodic GN Model for Space-Division Multiplexing With Strong Mode Coupling," *J. Light. Technol.,* vol. 40, no. 10, pp. 3263–3276, 2022.

[40] R. Dar, M. Feder, A. Mecozzi, and M. Shtaif, "Pulse collision picture of inter-channel nonlinear interference in fiber-optic communications," *J. Light. Technol.,* vol. 34, no. 2, pp. 593–607, 2016.

[41] Q. Zhang and M. I. Hayee, "Symmetrized Split-Step Fourier Scheme to Control Global Simulation Accuracy in Fiber-Optic Communication Systems," *J. Light. Technol.,* vol. 26, no. 2, pp. 302–316, 2008.

[42] K. -P. Ho and J. M. Kahn, "Frequency Diversity in Mode-Division Multiplexing Systems," *J. Light. Technol.,* vol. 29, no. 24, pp. 3719–3726, 2011.

[43] C. Lasagni, P. Serena, A. Bononi, A. Mecozzi, and C. Antonelli, "Dependence of nonlinear interference on mode dispersion and modulation format in strongly-coupled SDM transmissions," *Opt. Express*, vol. 31, no. 11, pp. 17122–17136, 2023.